Revista de Chimie
https://revistadechimie.ro
https://doi.org/10.37358/Rev.Chim.1949

Preparation and Modification of Graphite-based and Coal-based Graphene and its Tribological Properties in Lubricants

XUWEI ZHAO[1], KAIBINUER AIERKEN[2], HALIDAN MAIMAITI[1*], LIRONG FENG[1], JIANZHAO BAO[1], JINYAN SUN[1]

[1]School of Chemical Engineering and Technology, Xinjiang University, Urumqi 830046, 666 Shengli Road, Tianshan District, Urumqi, Xinjiang, China

[2]Xinjiang Uygur Autonomous Region Product Quality Supervision and Inspection Institute, Urumqi, 830011, 188 Hebei East Road, Xinshi District, Urumqi, China

***Abstract**: Graphite-based graphene oxide (GO) and coal-based graphene oxide (GO/SiO_2, which we call graphene oxide/SiO_2 because the surface of the resulting coal-based GO is linked with SiO_2 from the coal structure) were prepared by the conventional Hummers oxidation method and ultrasound-assisted Hummers oxidation method, respectively, using natural graphite powder and Xinjiang Wucaiwan coal as carbon sources. Furthermore, the structures of the two were studied comparatively. Afterwards, the two lamellar structure products were hydrophilically modified with octadecylamine and dicyclohexylcarbodiimide by a hydrothermal method. And then, added these products (graphite-based GO-ODA and coal-based GO/SiO_2-ODA) to No.32 cycloalkyl base oils in order to comparatively investigated their tribological properties as lubricant additives. The results showed that the dispersion stability of coal-based GO/SiO_2 in the lubricant was significantly better than that of graphite-based GO; meanwhile, the tribological performance of GO/SiO_2-ODA in the lubricant better than that of graphite-based GO-ODA due to the surface linkage of coal-based GO/SiO_2 with SiO_2 particles. After 1 h - long grinding in a four-ball friction test, the lubricant friction coefficient of 0.03 wt% coal-based GO/SiO_2-ODA oil reached a minimum of 0.118, which reduced 58.1% compared to pure base oil and reduced 2.8 times compared to the counterpart using graphite-based GO-ODA under the same experimental conditions.*

***Keywords**: graphite-based GO, coal-based GO/SiO_2, lubricant additives, dispersion stability, tribological properties*

1.Introduction

Since the industrial revolution, technology rapidly develops and results in an increasing scarcity of non-renewable energy sources [1]. In addition, a large proportion of energy is consumed to overcome friction in mobile mechanical systems, and data shows that approximately one third of human primary energy is lost owing to friction [2]. At the same time, "friction" is also responsible for more than 70% of equipment damage [3]. Friction is everywhere in our daily lives, for example, the speeding cars on the street, the machinery in factories, as well as every sliding, rolling or rotating contact interface. If friction is not effectively reduced or controlled, it not only accelerates the consumption of energy materials, but also leads to high abrasion, low life expectancy and low reliability of machinery.

In production and in life, lubricants are often used to reduce friction between moving parts [4]. Until now, numerous research focus on the nature and role of lubricants, which solves this wear problem in many important components in machinery and equipment [5-7]. In particular, nano-additives can significantly improve lubricants so as to reduce losses and enable the normal operation of equipment [8]. This is due to the high oil film strength of nano-additives which can effectively repair the worn parts of machinery.

Common nano-additives include carbon-based nanomaterials such as graphite and graphene (GO) [9], inorganic salts such as calcium borate and magnesium borate [10], soft nano metals such as copper and nickel [11], as well as other organic polymers such as organic borides [12].

**email: m15899160730@163.com*

Among them, GO, as a typical representative of two-dimensional carbon materials, become a hot topic in the lubrication field.

It has been found that GO is a two-dimensional lamellar material which has a honeycomb-like structure. Since its low friction coefficient, excellent mechanical properties and stable physical and chemical properties, it becomes an ideal material for abrasion and loss reduction [13-15], which can not only independently constitute a solid lubricating film between the friction pairs, but also be used as an efficient additive in lubrication products, considering the effect of wear and loss reduction and stabling suspension lubricant.

Similarly to GO, Nano-SiO_2 can be coated on the surface of GO to form GO/SiO_2. And this replacement can greatly reduce the fold and agglomeration degree of GO, and therefore, fully manifest its excellent mono-disperse properties [16]. For example, Pengfei Guo et al [17] prepared a novel nanomaterial named aminated silica modified graphene oxide (SAG), which combines the layered nanomaterial graphene oxide (GO) and the nanoparticles hydrophilic nano-silica (SiO_2) by 3-amino-propyltriethoxysilane (APTES). The wear rate of the ball lubricated by SAG at a concentration of 0.05% has a dramatic decrease, up to 78.3% compared with that of lubricated by pure water.

It was found that coal-based graphene oxide/silica (GO/SiO_2) nanocomposites could be synthesized in only one step by a modified Hummers oxidation method using Xinjiang Wucaiwan coal as raw material [18,19]. This composite material has the same two-dimensional lamellar structure as GO, and keeps the high thermal conductivity as well as high mechanical properties advantages of nano-SiO_2 and GO. Therefore, coal-based GO/SiO_2 may be served as lubricant additives after lipophilic treatment, when it exhibits better frictional properties through additive or synergistic effects of these two nanomaterials.

Hence, this thesis produced graphite-based GO and coal-based GO/SiO_2 through a modified ultrasound-assisted Hummers oxidation method where natural graphite powder and Xinjiang Wucaiwan coal acts as carbon sources, respectively. The structure and properties of these two materials generating from different carbon sources were investigated, and in the meantime, they were studied as lubricant additives of No.32 cycloalkyl base oil after lipophilicity modification, including their dispersion stability in lubricants and the effect of their addition amount on the tribological performance of lubricants. Finally, the mechanism why the coal-based GO/SiO_2 can improve the tribological performance of lubricants more efficiently was revealed.

2. Materials and methods

2.1. Materials and reagents

The materials and reagents for the study included: The coal sample used here is obtained from the Wucaiwan coal mine at China's Xinjiang Zundong coal field. The sample is grinded and filtered through a 200# mesh sieve, followed by a 4 h desiccation at 100°C. Natural graphite powder was provided by Tianjin Shengao Chemical Reagent Company Limited; No. 32 cycloalkyl base oil, supplied by Xinjiang Fokker Oil Company Limited Natural graphite powder was provided by Tianjin Shengao Chemical Reagent Company Limited; No. 32 cycloalkyl base oil, supplied by Xinjiang Fokker Oil Company Limited. Ferric chloride ($FeCl_3$, analytical pure), potassium permanganate ($KMnO_4$, analytical pure), boric acid (H_3BO_3, analytical pure) and hydrofluoric acid (HF, 40.0 wt%, analytical pure), P Hydrogen peroxide (H_2O_2, 30wt%), sulfuric acid (H_2SO_4, 98.2 wt%), hydrochloric acid (HCl, 36.5 wt%), Potassium persulphate ($K_2S_2O_8$), phosphorus pentoxide (P_2O_5), sodium nitrate ($NaNO_3$), octadecyl-amine ($C_{15}H_{39}N$), dicyclohexylcarbodiimide (DCC), all analytical pure, market sales.

2.2 Additive sample preparation

2.2.1. Graphite-based graphene oxide (GO)

The graphite-based GO was prepared by the ultrasound-assisted Hummers oxidation method, and the experimental steps were as follows.

(i) Low-temperature reaction: 1 g natural graphite powder and 0.5 g of sodium nitrate were sonicated and dispersed in 30 mL H_2SO_4 for 1 h (H_2SO_4 was placed in an ice-water bath and the temperature is

lower than 5°C). Next, add 3 g $KmnO_4$ slowly and turn off the sonication. And then, stir this solution for 1 h and keep the temperature no higher than 10°C. After the low-temperature reaction, a dark green dispersion can be obtained.

(ii) Medium-high temperature reaction: transfer the reaction solution to a constant temperature oil bath at 35°C and stir for 30 min, after that, there is an obvious purple-red colour in the inner wall of the beaker. Subsequently, add the above reaction solution slowly to 100 mL deionized water, transfer it to a constant temperature oil bath at 95°C and stir for 30 min to obtain a brown reaction solution. Next, add 200 ml deionized water to terminate the reaction, and add 30% H_2O_2 to remove the excess $KMnO_4$. At last, stir this solution for 30 min and leave it to stand.

(iii) Purification process: centrifuge the above reaction solution (at 8000 r/min^{-1} for 5 min), and remove the supernatant (wash the precipitate in the centrifuge tube repeatedly with deionised water until the supernatant of the tube reached neutral and the lower layer of the precipitate changed from light brown to viscous brown-black). Next, take this precipitate, disperse it in deionised water, sonicate for 40 min, and centrifuge (2500 r/min^{-1} for 30 min). After centrifugation, the upper brown liquid is graphene oxide dispersion. Finally, this dispersion was put into a constant temperature drying oven at 80°C for 12 h to obtain a black flake product, which is the target graphite-based GO product.

2.2.2. Coal-based graphene oxide / silica (GO/SiO_2)

A modified ultrasound-assisted Hummers oxidation method [20] was used to prepare coal-based GO/SiO_2, and compared to the graphite-based GO, there are some additional steps such as graphitization, pre-oxidation of coal and so on:

(i) weighed, ground, and mixed the pulverised coal, $FeCl_3$ and H_3BO_3 (mass ration 16:3:1) in an agate mortar, and then placed it in a tube furnace (rated at 1000°C), programmed temperature to 950°C for 5 h under N_2 ambience (60 mL/min), after that, cool naturally to room temperature under N_2 atmosphere to obtain graphitised pulverised coal.

(ii) dispersed 8 g pretreated coal sample in 30 mL mixed H_2SO_4 solution which contains 8 g $K_2S_2O_8$ and 8 g of P_2O_5 , stir at room temperature for 3 h and stir at 80°C for 6 h, then cool down, filter, wash to remove acid and salt, and dry at 80°C to obtain the pre-oxidation product.

(iii) slowly add the above pre-oxidised pulverised coal to 180 mL concentrated H_2SO_4 (H_2SO_4 was placed in an ice-water bath and keep the temperature not more than 5°C) and stirred for 30 min, then add 24 g $KMnO_4$ in multiple portions (ultrasonic ice bath (40 kHz, 200 W)) and stir for 30 min (during this stirring, the system temperature was controlled below 10°C). Then, raised the water bath temperature to 35°C and continued stirring for 4 h. Afterwards, added 30 mL deionised water every 5 min for three times, stirred for 30min, and subsequently, terminated this reaction by adding 1 L deionised water. Finally, add 30 % H_2O_2 to remove excess $KMnO_4$, stir for 30 min and leave to stand. Wash, filter, and dry at 80°C for 6 h to obtain black powder, which is the target coal-based GO/SiO_2 product.

2.2.3. Preparation of graphite-based GO and coal-based GO/SiO_2 modified lubricants

(1) Lipophilic modification of additives

After drying, 0.1 g of graphite-based GO (or coal-based GO/SiO_2) was ultrasonically dispersed in 120 mL of deionized water, 0.5 g of octadecylamine and 0.1 g of dicyclohexylcarbodiimide were added and the reaction was stirred at room temperature for 30 min. After that, the reaction was heated to 120°C and refluxed for 12 h. After the reaction, the black solids in the reaction solution were filtered out and washed with deionized water and ethanol respectively for three times and dried at 80°C for 24 h. The graphite-based GO (or coal-based GO/SiO_2) was washed three times with deionized water and ethanol, and dried at 80°C for 24h to obtain GO-ODA (or coal-based GO/SiO_2-ODA), a lipophilic modified product of graphite-based GO (or coal-based GO/SiO_2).

(2) Formulation of modified lubricants

The unmodified GO and GO/SiO_2, as well as the modified GO-ODA and GO/SiO_2-ODA were added into the No.32 cycloalkyl base oil respectively and ultrasonicated to obtain a uniformly dispersed additive/lubricant system.

2.3. Characterization

The morphological structure of the sample was observed using H-600 transmission electron microscope (TEM, HRTEM). Field emission scanning electron microscope images of each sample were obtained by SU1080 electron microscope (SEM). The elemental analysis of each sample was carried out by a HITACHI-SU8010 EDS spectrometer (acceleration voltage: 5 kV, scan distance 8 mm). X-ray diffraction (XRD) results for each sample were obtained by using M18XHF22-SRA X-ray diffractometer (experimental conditions: Cu Kα radiation λ=0.154056 nm, scan range: 2θ=10-80°). Raman spectra of the samples were collected by a Raman spectrometer (BRUKER VERTEX 70). The FTIR spectrum of the samples were obtained by a Fourier transform infrared spectrometer (FTIR, Bruker-EQUINOX 55). The surface chemical properties of the samples were detected by an X-ray photoelectron spectrometer (XPS, ESCALAB 250, number of scans: 3, number of energy steps: 1001, energy step size: 0.05 eV). After the four-ball friction and wear test, the steel balls were sonicated in petroleum ether for 30 min, dried sufficiently and then the surface morphology of the wear marks was observed with an Olympus BX60M optical microscope (OM), and the diameter of the wear marks was calibrated with a wear mark measurement software.

2.4. Friction and wear experiments with graphite-based GO, coal-based GO/SiO_2 and their lipophilic modified products as lubricant additives

Graphite-based GO, coal-based GO/SiO_2 and their lipophilic modification products GO-ODA and GO/SiO_2-ODA were used as lubricant additives and then added to No. 32 cycloalkyl base oil respectively before being subjected to frictional wear tests in the MRS-1J mechanical four-ball long-time anti-wear tester shown in Figure 1 (test method according to SH/T 0189-92).

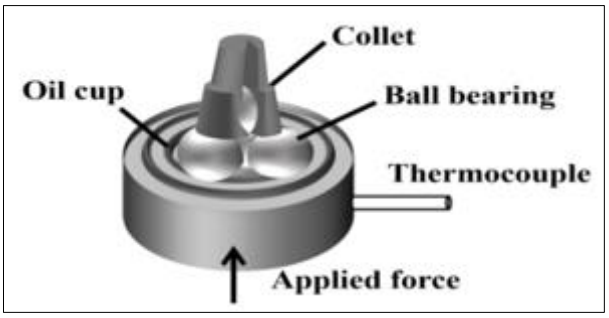

Figure 1. Schematic diagram of four-ball testing machine

The diameter of the balls used was 12.7 mm and the material was CGr15, with a hardness between HRC 61 and 66. The test speed was set at 1450 r/min, the load at 196 N, the test time at 3600 s and the temperature at room temperature. After the experiment, the mean friction factor was read and the balls were cleaned and dried, and the diameter of the wear spots was read under an optical microscope.

3. Results and discussions

3.1. Microstructure of graphite-based GO and coal-based GO/SiO_2

To understand the morphological structures of graphite-based GO and coal-based GO/SiO_2, TEM and SEM tests were carried out, and the results are shown in Figure 2.

Figure 2A and 2B are TEM and SEM results of graphite-based GO, respectively. It can be seen that our prepared graphite-based GO has a two-dimensional nanosheet structure, close to a single atomic

layer, and its edge are warped or curled. From the HRTEM results shown in Figure 2C, we can observed that the lattice spacing of graphite-based GO is 0.229 nm, which belongs to the unique GO(001) lattice of the graphite-based GO. This result is consistent with other literature reports [21], indicating that the graphene oxide can be effectively exfoliated from natural graphite using the modified Hummers method.

Figure 2D and 2E show the TEM and SEM images of coal-based GO/SiO_2, respectively. It is obvious that coal-based GO/SiO_2 also has a two-dimensional nanosheet structure, and these nanosheets are coated with dense particulate matter (thought to be SiO_2 layers by subsequent characterisation). The edges of the coal-based GO/SiO_2 appear to be flat and smooth. There is some wrinkles in the middle portion but not folding, which is clearly due to the presence of SiO_2 particles. From the HRTEM image shown in Figure 2F, the surface of the coal-based GO/SiO_2 nanosheets has distinct lattice stripes with a spacing of both 0.229 nm and 0.257 nm, which belongs to the GO (001) and SiO_2 (110) lattices, respectively [22]. Therefore, we think the coal-based GO/SiO_2 is formed by coating the GO surface with SiO_2 particles.

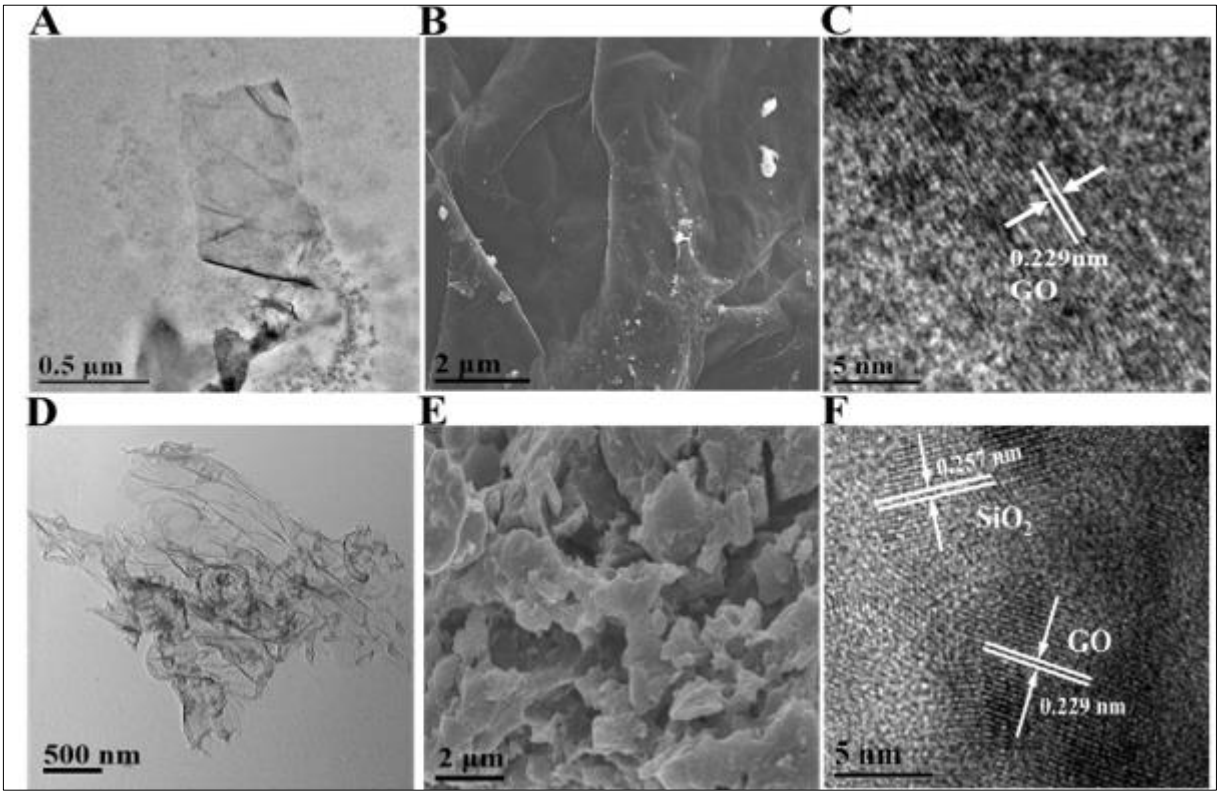

Figure 2. The TEM (A), SEM (B) and HRTEM (C) image of graphite-based GO; The TEM (D), SEM (E) and HRTEM (F) image of coal-based GO/SiO_2

Comparing the morphology of these two material, both are in the form of lamellae. The graphite-based GO lamellae are thin, smooth and soft. The warped edges and raised folds of the lamellae can be clearly seen. While the coal-based GO/SiO_2 is thicker, rougher, and coating with abundant particles. Furthermore, we speculate that the coal-based GO/SiO_2 surface should have greater mechanical strength and a relatively stable C-C bond structure, making it more suitable to use as a lubricant additive.

In order to know the composition of the prepared samples, we carried out EDS tests on graphite-based GO and coal-based GO/SiO_2, and SEM-Mapping tests on coal-based GO/SiO_2. As shown in Figure 3A and 3B, the content of C and O in graphite-based GO was 51.06 % and 48.94 % respectively. The main elements of the coal-based GO/SiO_2 were C, O and Si, with 65.73, 30.2 and 2.06 % content, respectively. Compared to graphite-based GO, the elemental content of C in coal-based GO/SiO_2 increased and the relative content of O reduced, while the element Si appears.

Figure 3C-F shows the SEM-Mapping results of coal-based GO/SiO_2. It is obvious that the coal-based GO/SiO_2 is a coiled sheet layer, and the C, O and Si elements distributed evenly. It indicates that O and Si elements are loaded on the surface of the GO sheet which is dominated by C elements. SiO_2 is uniformly loaded on the GO surface.

To further investigate the structural characteristics of graphite-based GO and coal-based GO/SiO_2, we have performed XRD, Raman and FTIR characterisation of both, and the results are shown in Figure 4.

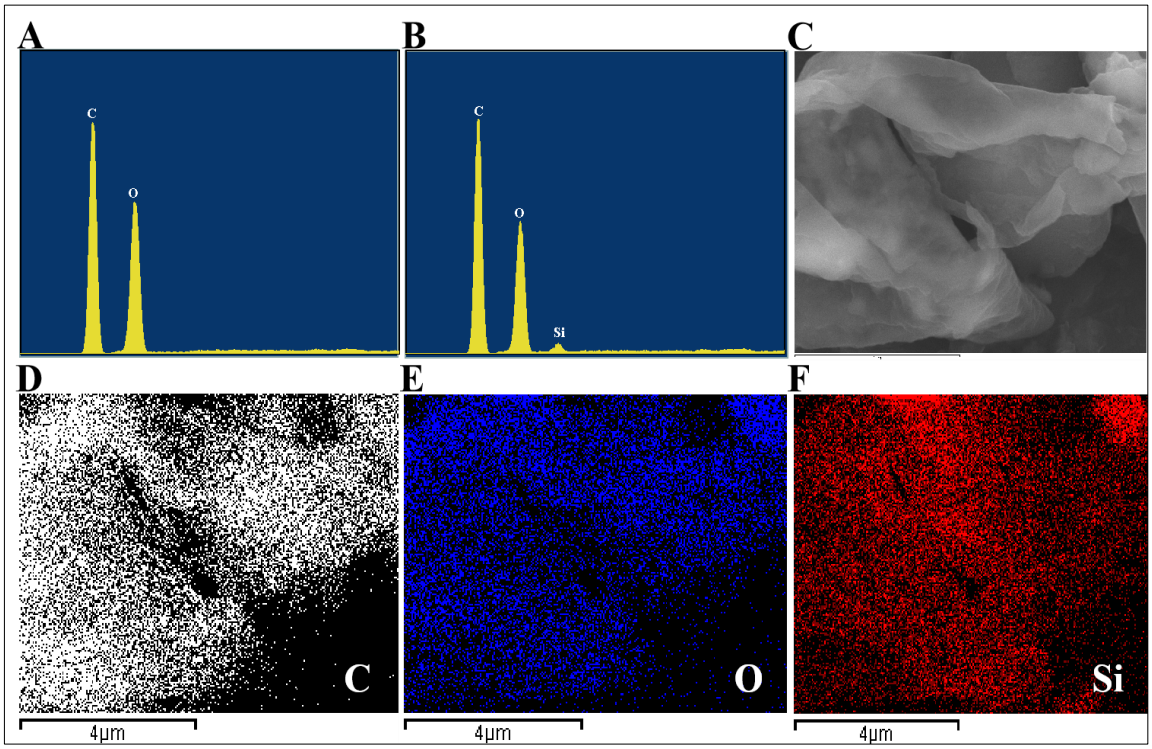

Figure 3. The EDS image of graphite-based GO(A) and coal-based GO/SiO_2(B); SEM-mapping image of coal-based GO/SiO_2(C-F)

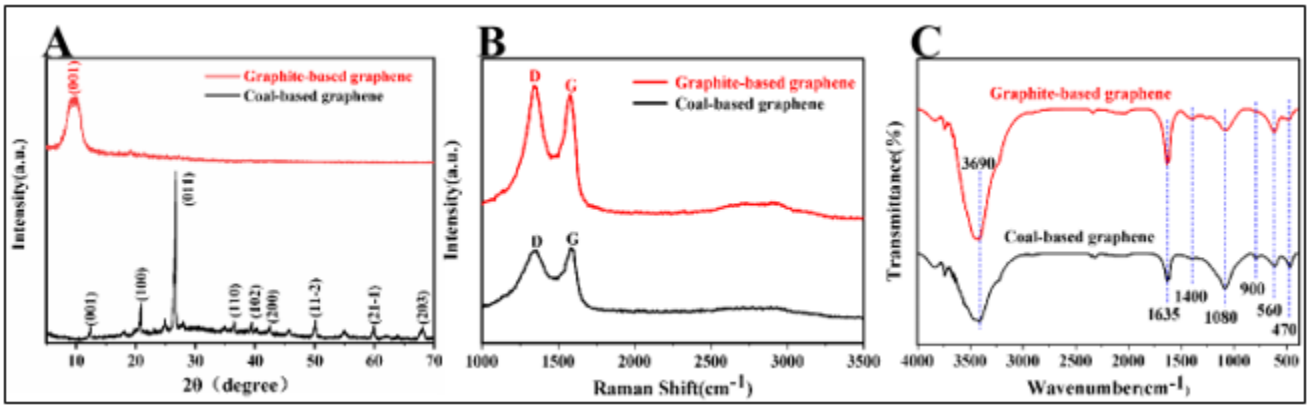

Figure 4. XRD (A), Raman (B) and FTIR (C) image of graphite-based GO and coal-based GO/SiO_2

XRD characterisation is an effective method to study the crystal structure. We have carried out XRD tests on graphite-based GO and coal-based GO/SiO_2 respectively and the results are shown in Figure 4A. The graphite-based GO shows a characteristic diffraction peak at $2\theta=10.2°$ corresponding to the (001) crystal plane of GO, which is consistent with the results reported in the literature [23]. At the same time, no impurity peaks appeared in the XRD spectrum of graphite-based GO, which indicates that we have successfully prepared graphite-based GO with high purity

The coal-based GO/SiO_2 shows a characteristic diffraction peak at 2θ = 12.3° corresponding to the (001) crystallographic plane of GO [24], and at 2θ = 20.8°, 26.5°, 36.5°, 39.5°, 42.4°, 50.1°, 59.9° and 68.1° corresponding to the (100), (011), (110), (102),(203), (200), (11-2), (21-1) and (203) crystallographic planes of SiO_2, respectively. This is consistent with the JCPDS (No. 77-106) standard data for trigonal crystalline SiO_2 [25], which indicates that the prepared coal-based GO/SiO_2 is formed by GO surface-linked SiO_2.

Comparing the XRD spectra of these two samples, the intensity of the GO (001) peaks of coal-based GO/SiO_2 is significantly weaker than that of graphite-based GO. This is due to the presence of SiO_2 on the surface of coal-based GO/SiO_2, which weakens the GO (001) characteristic diffraction peaks peak. Furthermore, the coal-based GO/SiO_2 also shows the corresponding SiO_2 characteristic diffraction peaks at 2θ = 20.8°, 26.5°, 36.5°, 39.5°, 42.4°, 45.7°, 50.1°, 54.8°, 59.9° and 68.1°. This result further indicates that the prepared coal-based GO/SiO_2 are formed by linking SiO_2 on the surface of coal-based GO.

Raman spectroscopy is an effective way of characterizing the extent of defects in carbonaceous nanomaterials, and we can obtain the distribution of sp^2 and sp^3 carbon in the structure, by comparing the ratio of the D band intensity to the G band intensity (I_D/I_G). (D and G band correspond to the sp^2 ordered carbon structure and sp^3 disordered carbon structure, respectively) [26]. Figure 4B show Raman results of graphite-based GO and coal-based GO/SiO_2.The graphite-based GO and coal-based GO/SiO_2 show a D-peak at 1350 cm^{-1} representing a structural defect in the carbon material, and a G-peak at 1581 cm^{-1} corresponding to the disordered vibration of the sp^3 carbon atoms. The peak intensity ratio (I_D/I_G) of the D and G peaks for graphite-based GO was calculated to be 1.06, while the I_D/I_G ratio for coal-based GO/SiO_2 was 0.95. This indicates that the prepared coal-based GO/SiO_2 has a high content of internal defects and a high degree of carbon tissue disorder.

To investigate the surface groups in graphite-based GO and coal-based GO/SiO_2, as well as the bonding type between SiO_2 particles and GO in coal-based GO/SiO_2we performed Fourier transform infrared characterisation (FTIR) of these two material, as shown in Figure 4C.

Both graphite-based GO and coal-based GO/SiO_2 show a peak at 3409 cm^{-1} representing the hydroxyl group vibration on the surface of the GO material [27]. But t the vibration peak intensity of coal-based GO/SiO_2 is weaker. Because Si-OH on the surface of the SiO_2 layer and oxygen-containing groups such as C-OH on the surface of the GO sheet layer formed Si-O-C bonds through dehydration condensation. This results in a bonding of the SiO_2 to the GO lamellae, leading to a significant reduction in the hydroxyl content of the GO/SiO_2 surface. Meanwhile, the absorption peaks of Si-O-Si and Si-O-C appeared at 470 cm^{-1}, 1084 cm^{-1}, 1400 cm^{-1} and 1638 cm^{-1} for coal-based GO/SiO_2 [28]. These peaks verify the presence of SiO_2 in GO/SiO_2. We believe that the SiO_2 in the GO/SiO_2 structure converted from silicates presenting in the coal structure under strong acid oxidation, and then condensed and dehydrated with oxygen-containing groups such as hydroxyl groups on the surface of the coal-based GO lamellae to form Si-O-C.

In order to further understand the chemical structure and formation mechanism of graphite-based GO and coal-based GO/SiO_2, we used XPS to analyze the various chemical bonds in graphite-based GO and coal-based GO/SiO_2 structures, as shown in Figure 5.

Figure 5A shows the full XPS spectra of graphite-based GO and coal-based GO/SiO_2. Both graphite-based GO and coal-based GO/SiO_2 display C1s and O1s peak at 284.6 eV and 532.1 eV, respectively. What's more, the coal-based GO/SiO_2 shows a extra peak corresponding to Si_2p at 103.4 eV, and the corresponding Si content is only 2.04 %, which is consistent with the EDS analysis.

The fitting curves of XPS spectra for C, O and Si peaks are shown in Figure 5B-5D, respectively. The C1s XPS spectrum (Figure 5B) illustrated four main peaks with the binding energy of 284.6 eV(C=C/C-C), 285.6 eV(C-OH), 286.8 eV(C-O) and 288.8 eV(C=O) [29], respectively. Among them, the number of C-OH and C-O bonds in coal-based GO/SiO_2 is smaller than that of graphite-based GO, and this result is consistent with the FTIR analysis. This is because the Si-OH on the surface of the SiO_2 layer and the C-OH on the surface of the GO sheet form Si-O-C bonds through inter-layer condensation and dehydration, resulting in a decreasing number of C-OH and C-O bonds in coal-based GO/SiO_2.

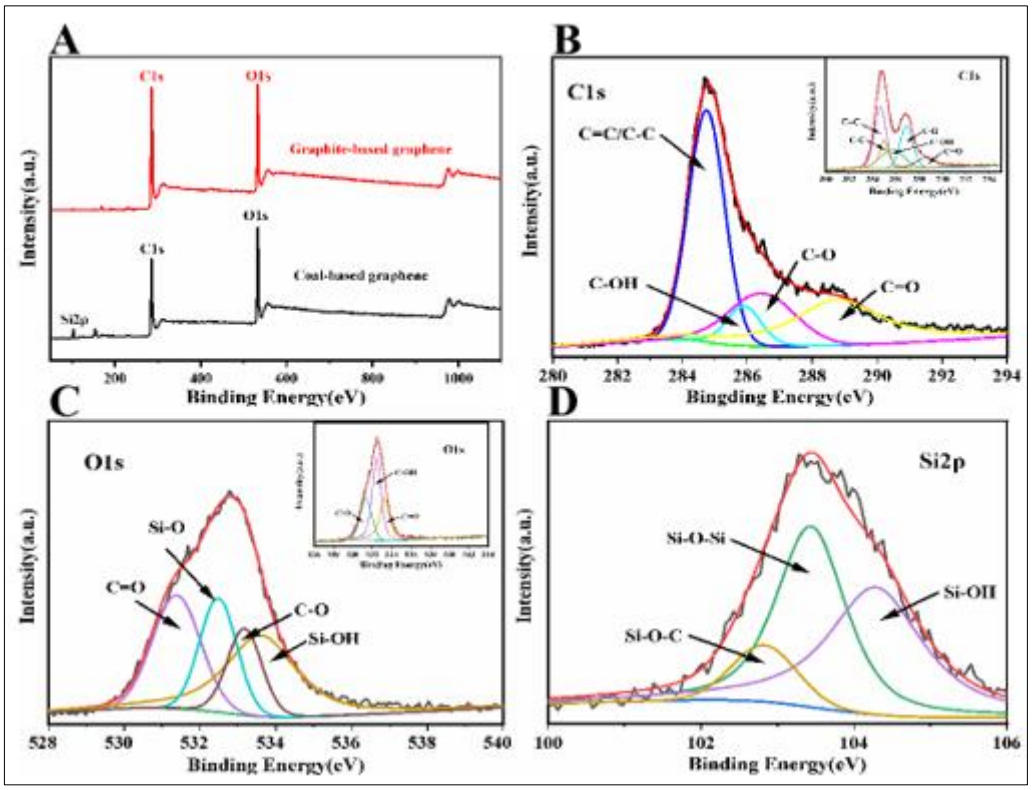

Figure 5. XPS (A-D) spectrum of coal-based GO/SiO_2 and graphite-based GO(insert)

The O1s XPS spectrum (Figure 5C) illustrated three peaks with the binding energy of 531 eV(C-O), 532.1 eV(C-OH) and 533.2 eV (C=O) [30], respectively. In addition, the coal-based GO/SiO_2 shows a extra characteristic peak at 533.8 eV corresponding to the Si-OH group. The Si_2p XPS spectrum (Figure 5D) illustrated three peaks with the binding energy of 102.1eV (Si-O-C), 103.3 eV(Si-O-Si) and 104.3 eV (Si-OH) [31], respectively.

From XPS tests, we believe that C-C/C=C, C-OH, C-O, C=O and O-C=O in coal-based GO/SiO_2 are derived from coal-based GO that stripped from the coal structure, while Si-O-Si and Si-O are derived from SiO_2 particles that obtained from the conversion of silicate species in coal. Furthermore, the presence of Si-O-C in the GO/SiO_2 structure proves that the SiO_2 particles are bonded to the GO by chemical bonding.

In conclusion, we believe that the additive effect of SiO_2 particles on surface of coal-based GO forming GO/SiO_2 achieves a complementary advantage to the strength of both. Thus, when coal-based GO/SiO_2-ODA is used as a lubricant additive, the lubricant has better anti-wear and friction-reducing properties.

3.2. Dispersion stability of graphite-based (GO) and coal-based graphene oxide/silicon dioxide (GO/SiO_2) in lubricants

According to the aforementioned method, the graphite-based GO and coal-based GO/SiO_2 were treated with lipophilic modification (denoted as GO-ODA and GO/SiO_2-ODA). To investigate the dispersion stability of these two materials in the lubricant and the effect of lipophilic modification, we added unmodified GO and GO/SiO_2, as well as modified GO-ODA and GO/SiO_2-ODA to No. 32 cycloalkyl base oil (formulated 0.03 wt% additive/lubricant dispersion system), respectively. The results are shown in Figure 6.

Figure 6A-6D show 1-4$^{\#}$ samples, 0-21days after ultrasonic dispersion, and 1-4# samples are ① The graphite GO/lubricant, ②coal-based GO/SiO_2/lubricant, ③graphite-based GO-ODA/lubricant and④ coal-based GO/SiO_2-ODA/lubricant systems, respectively. It can be seen that on the day of ultrasonic dispersion, the above four samples were uniformly dispersed in No. 32 cycloalkyl base oil. After 7 days

of resting, precipitates started to appear in the graphite-based GO/lubricant system. After 14 days of resting, both graphite-based GO/lubricant and coal-based GO/SiO_2/lubricant systems generated precipitates. After 21 days of resting, these samples showed precipitates except for coal-based GO/SiO_2-ODA/lubricant system which maintained the dispersion stability. The above results show that the dispersion stability of coal-based GO/SiO_2 in lubricants is better than that of graphite-based GO; because grafted long-chain alkanes have a positive lipophilic dispersion effect on coal-based GO/SiO_2.

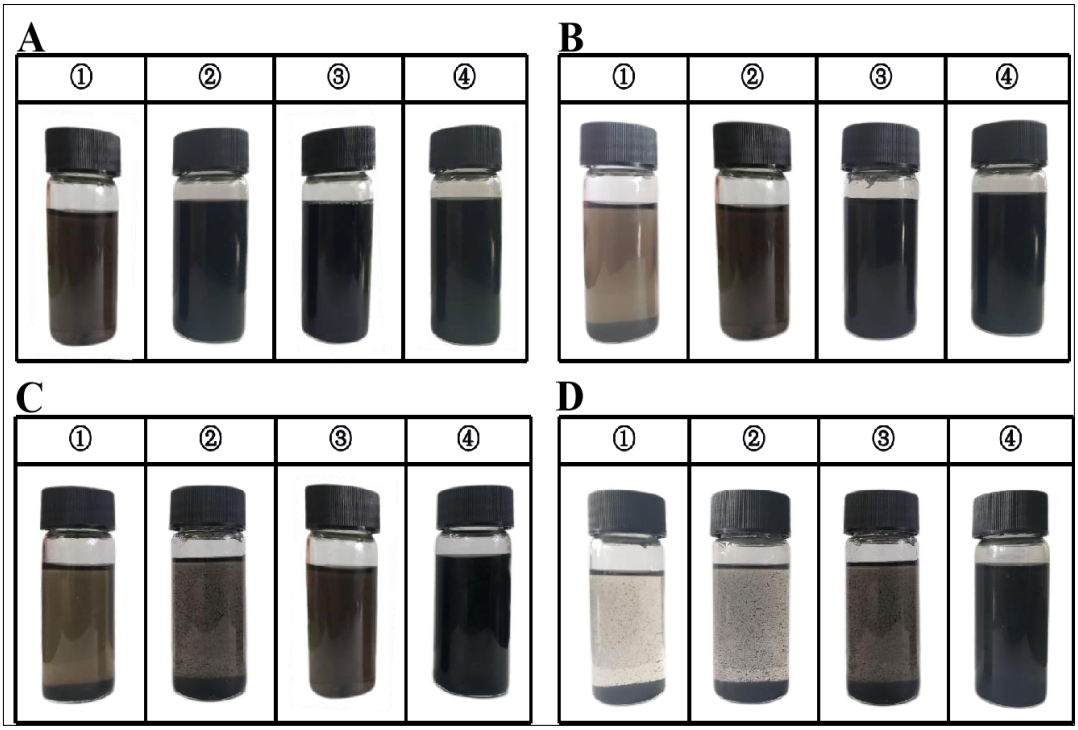

Figure 6. Dispersion stability of GO-ODA/lubricating oil and GO/SiO_2-ODA/lubricating oil. (A) The day after ultrasonic dispersion; (B) 7 days after ultrasonic dispersion; (C) 14 days after ultrasonic dispersion; (D)21 days after ultrasonic dispersion

In order to study the effects of graphite-based GO and coal-based GO/SiO_2 on the light transmission properties of lubricating oil, the absorbance curves of GO-ODA/lubricating oil (A) and GO/SiO_2-ODA/lubricating oil (B) systems with different concentrations were measured by spectrophotometer from 280 nm to 600 nm, and the results are shown in Figure 7A-7B. The trends of these two curves are similar. The absorbance of GO-ODA/Lubricant (B) at wavelengths between 280 and 320 nm is relatively strong, and the absorbance decreases as the wavelength extends gradually, showing a relatively weak characteristic absorption peak near 342 nm. Then the absorbance decreases again and finally tends to level off. However, the absorbance of the GO/SiO_2-ODA/lubricant system is greater than that of the GO-ODA/lubricant system at the same GO-ODA and GO/SiO_2-ODA additions, which again indicates that the dispersion stability of coal-based GO/SiO_2-ODA is better than that of graphite-based GO-ODA. The reasons after this phenomenon are that: (1) the regular SiO_2 loading onto the coal-based GO surface can inhibit the agglomeration of GO [32], thus improving its dispersion stability in the lubricant; (2) SiO_2 itself has good dispersibility in the lubricant [33], which can also improve the dispersion stability of coal-based GO/SiO_2 in the lubricant.

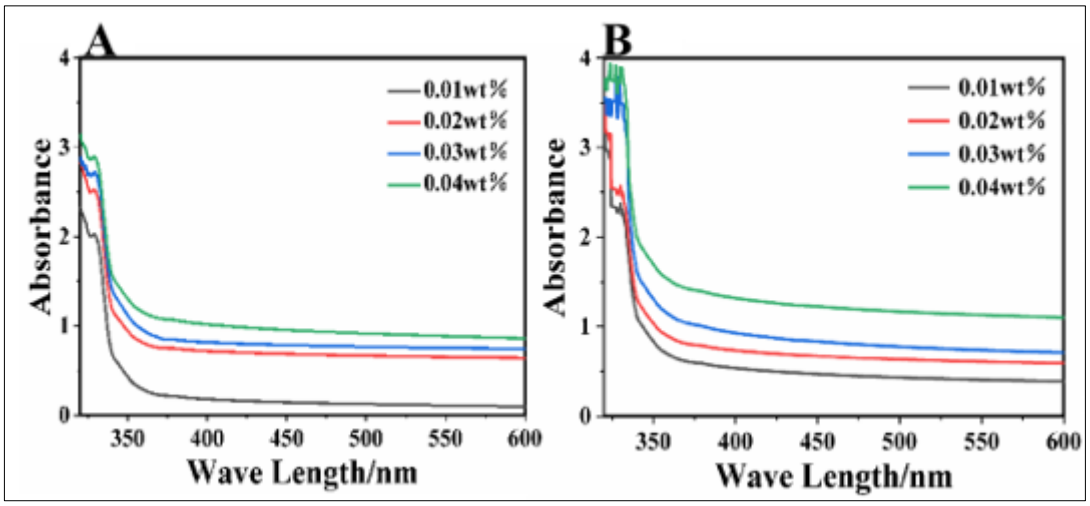

Figure 7. UV-Vis absorption spectra and absorbance-concentration relationships of GO-ODA/lubricating oil (A) and GO/SiO_2-ODA/lubricating oil (B)

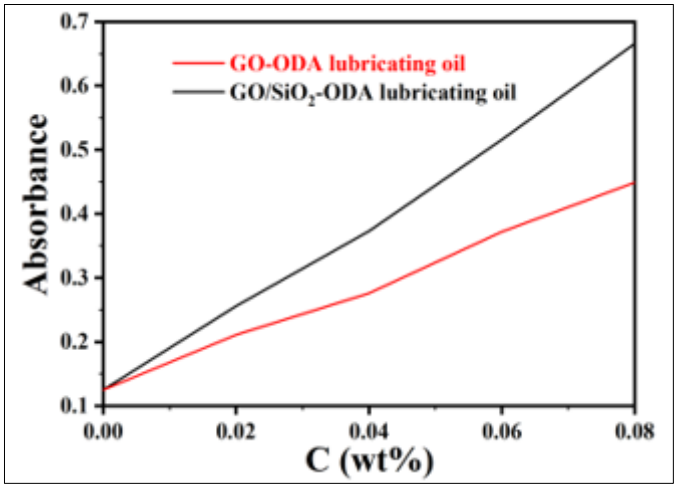

Figure 8. UV-Vis absorption spectra and absorbance-concentration relationships of GO-ODA/lubricating oil and GO/SiO_2-ODA/lubricating oil

The absorbance values of additive/lubricant systems are related to the dispersion stability of the additives; and the higher the absorbance of the system, the better the dispersion stability of the additives [34]. To further demonstrate the dispersion stability of coal-based GO/SiO_2 in lubricants, we prepared graphite-based GO-ODA/lubricant and coal-based GO/SiO_2-ODA/lubricant systems with different concentrations, and tested their absorbance at 600 nm where the absorbance tends to stabilize after one week of storage. The absorbance of the additive/lubricant dispersion system were plotted in Figure 8. This image shows that the absorbance of the GO/SiO_2-ODA/lubricant system was greater than graphite-based GO-ODA/lubricant system in the detection range (0~0.08 wt%), which further indicates that coal-based GO/SiO_2 has better dispersion stability than graphite-based GO.

What is more, the absorbance of both the GO-ODA/lubricant and GO/SiO_2-ODA/lubricant systems is linearly related to the concentration of the additives (GO-ODA and GO/SiO_2-ODA), which shows good compliance with Lambert's law in the detection concentration range [35]: the absorbance of light is proportional to the number of molecules producing in the light path, which means the absorbance of a substance is proportional to the concentration of this absorbing substance. Therefore, we believe that the absorbance-concentration curve shown in Figure 8 can be used as a standard curve to analyze the additive/lubricant. Thus, the absorbance of the additive/lubricant dispersion system prepared in this

experiment can indirectly prove the dispersion stability of the additive (GO-ODA or GO/SiO_2-ODA) in the lubricant.

3.3. Tribological properties of graphite-based (GO) and coal-based graphene oxide/silicon dioxide (GO/SiO_2) in lubricants

The friction coefficients of GO-ODA/lubricant and GO/SiO_2-ODA/lubricant were determined by the aforementioned test methods and the results are shown in Figure 9A, B.

Figure 9A shows that the system friction factor reduced approximately 11.0 %, 12.6 %, 30.9 % and 3% when GO-ODA is added at 0.01 wt%, 0.02 wt%, 0.03 wt% and 0.04wt%, respectively. For GO/SiO_2-ODA (Figure 9B), this friction factor reduced by approximately 29%, 31.2%, 58.1% and 14.7%, when containing 0.01wt%, 0.02wt%, 0.03wt% and 0.04wt% GO/SiO_2-ODA. Clearly, in the tested concentration range (0-0.04wt%), as the amount of GO-ODA or GO/SiO_2-ODA increases, the friction coefficient of the additive/lubricant system first decreases and then increases. And the best tribological performance of the additive/lubricant system is achieved when the amount of GO-ODA or GO/SiO_2-ODA reaches 0.03wt%.

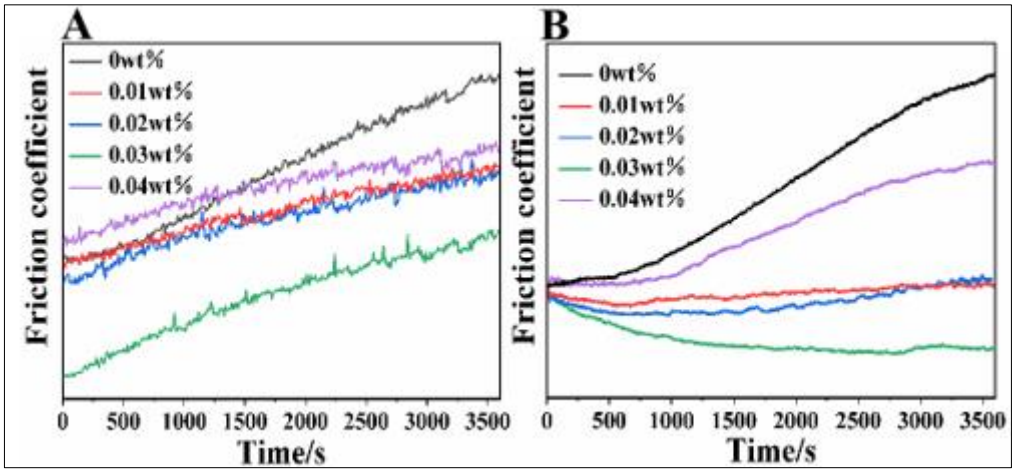

Figure 9. The relationship between the friction coefficient and additive concentration of GO-ODA/lubricating oil and GO/SiO_2-ODA/lubricating oil

We believe that the GO/SiO_2-ODA (or GO-ODA) micro-nanosheets which have better mechanical properties and ductility will fill in the contact interface of the friction substrate, forming a lubricating layer that avoids direct contact with other bumps on the friction substrate. Hence, the friction coefficient will obviously drop. At the same time, the flash temperature generated during the friction process can generate tribological reaction between the additive/lubricant and the friction substrate, so that the additive sheet lamellar structure will release interlayer domain active groups during the interlayer sliding. For example, when GO/SiO_2-ODA acts as additive, sassafras sub sliding layer will produce SiO_2, SiC and other active substances. These active groups produce reaction with the friction substrate, generate repair-coating, fill the defects of this friction surface, and thus improve the surface hardness reducing surface abrasion.

When the content of GO-ODA or GO/SiO_2-ODA reached 0.4wt%, the reduction in the friction coefficient increases (the friction factor of the GO-ODA/lubricant system only reduced 3%, and the counterpart of the GO/SiO_2-ODA/lubricant system is only 32.7%). We believed that these additive cannot cover the surface uniformly during the whole friction process due to excessive addition of GO-ODA or GO/SiO_2-ODA. They may accumulate between the friction pairs, disrupting the continuity of the oil film and leading to deterioration of the friction performance. Furthermore, excessive GO-ODA or GO/SiO_2-ODA may agglomerate with the tiny friction chips at the friction surfaces, making the friction surface wear increased.

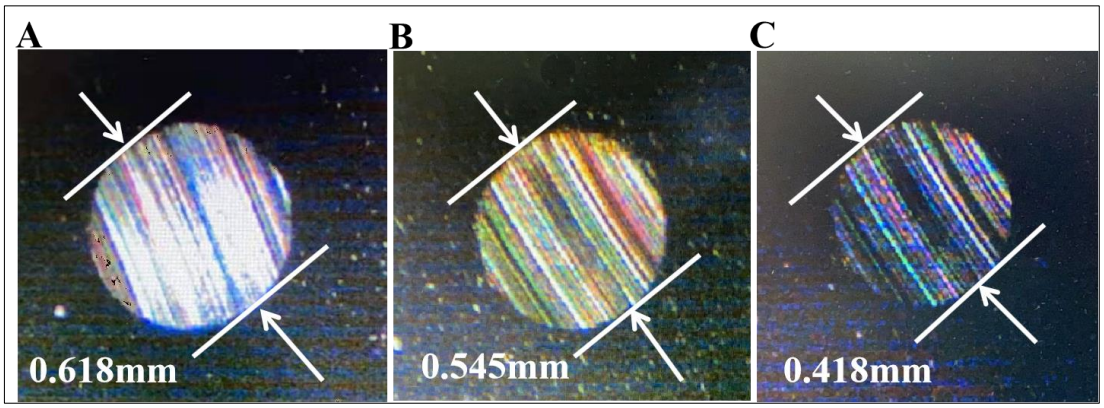

Figure 10. Wear scar diameters of pure lubricating oil (A), 0.03wt% GO-ODA/lubricating oil (B) and 0.03wt% GO/SiO_2-ODA/lubricating oil (C)

Figure 10A-10C show the wear spot diameter and surface profile of the steel balls after four ball friction tests for pure lubricant, GO-ODA/lubricant with 0.03 wt% and GO/SiO_2-ODA/lubricant systems, respectively. The smallest spot diameter is 0.418 mm observed at 0.03% GO/SiO_2-ODA (Figure 10C), which is approximately 33.7 % less than that of the pure lubricant (Figure 10A, spot diameter of 0.618). For the same content GO-ODA/lubricant, the spot diameter is 0.545 mm (Figure 10 B), and there is an 13.5 % reduction compared to pure lubricant. This result is consistent with the above friction factor variation pattern. In the meantime, it can be seen that the additive/lubricant system containing 0.03 wt% GO/SiO_2-ODA has significantly effect on reducing and lightening wear marks on the steel ball surface. This phenomena demonstrates the excellent wear reduction performance of GO/SiO_2-ODA as an additive to the lubricant.

Figure 11A and 11B show the SEM results of the microscopic surfaces of the steel ball wear spots after the four-ball friction test for 0.03 wt% GO-ODA/lubricant and 0.03 wt% GO/SiO_2-ODA/lubricant, respectively. It can be seen that in the four-ball friction test, GO-ODA and GO/SiO_2-ODA formed a protective film on the surface of the friction substrate, which isolated the direct contact between the upper and lower raised samples, resulting in a lower friction coefficient of the additive/lubricant. However, the protective film formed by the graphite-based GO-ODA/lubricant system on the steel ball surface was completely broken after test, but this protective film by the coal-based GO/SiO_2-ODA/lubricant system still existed. This results indicates that the protective film formed by the coal-based GO/SiO_2-ODA/lubricant on the steel ball surface was mechanically stronger, and possessed better anti-wear and friction-reduction properties. Due to coal-based GO/SiO_2 linked with SiO_2 particles at its surface, the additive effect on the strength of both achieves a complementary advantage. So the lubricant has better anti-wear and friction-reducing properties when coal-based GO/SiO_2-ODA acts as lubricant additive.

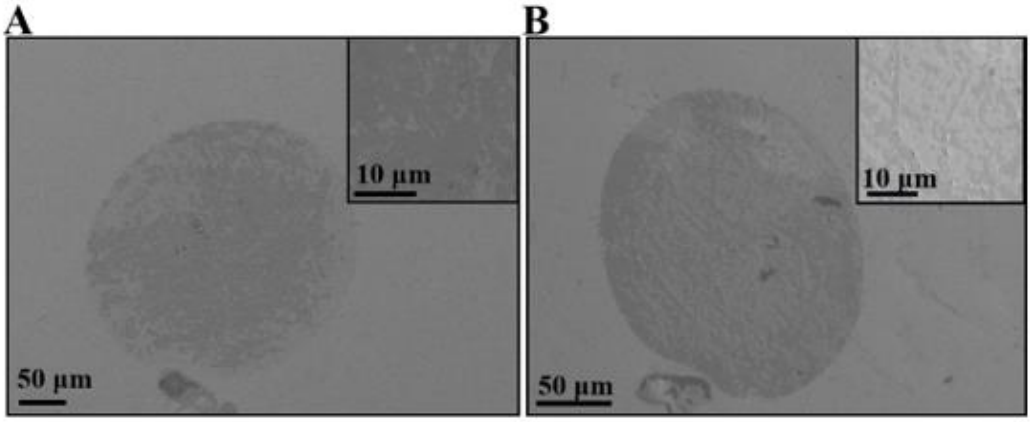

Figure 11. SEM images of the wear scar surface of steel balls for 0.03wt% GO-ODA/lubricating oil (A) and 0.03wt% GO/SiO_2-ODA/lubricating oil (B)

4. Conclusions

Graphite-based graphene oxide (GO) was prepared by the conventional Hummers oxidation method using natural graphite as raw material. Meanwhile, coal-based graphene oxide/silica (GO/SiO_2) nanosheets with the conventional graphene two-dimensional layer structure were prepared by ultrasound-assisted Hummers oxidation method. Here, coal is from Wucaiwan coal mine in Xinjiang as the carbon source, the GO flakes is stripped from graphite-like aromatic core of the coal structure, and SiO_2 particles produced by the oxidation of silica salts in the coal which linked to the surface of coal-based GO flakes. Furthermore, the structural characteristics of graphite-based GO and coal-based GO/SiO_2 were comparatively investigated.

We also produced lipophilic graphite-based GO-ODA and coal-based GO/SiO_2-ODA by the hydrothermal reactions grafting octadecyl amines onto graphite-based GO and coal-based GO/SiO_2, respectively. To comparatively study their dispersion stability in lubricants and the morphological properties of the additive/lubricant system, they were dispersed in No. 32 cycloalkyl base oil in comparison. The results showed that the dispersion stability and frictional properties of coal-based GO/SiO_2 in the lubricant was significantly better than that of graphite-based GO, due to the linked SiO_2 particles. After 1 h - long grinding in a four-ball friction test, the lubricant friction coefficient of 0.03 wt% coal-based GO/SiO_2-ODA oil reached a minimum of 0.118, which reduced 58.1 % compared to pure base oil and reduced 2.8 times compared to the counterpart using graphite-based GO-ODA under the same experimental conditions.

Acknowledgements： The authors are grateful for the financial support of the National Natural Science Foundation of China (21862020).

References

1.KENETH H., PETER A., et al., Global energy consumption due to friction in trucks and buses, Tribology International, **78**, 2014, 94-114.
2.FONTAINE J., DONNET C., Superlow Friction of a-C:H Films: Tribochemical and Rheological Effects, Superlubricity, **17**, 2017, 273-294.
3.RAPOPORT L., BILIK Y., Hollow nanoparticles of WS_2 as potential solid-state lubricants. Nature. **387**, 2012, 791-793.
4.KALIN M., Designing Tribological Interface for Efficient and Green DLC Lubrication: The Role of Coatings and Lubricants, Tribology Online, **7**, 2012, 112-118.
5.WAN FM., KHAN AA., et al., Sliding Friction Behavior of Sintered Ni-Cr Composites with Solid Lubricants[J], Key Engineering Materials, **875**, 2021, 272-279.
6.BOYDE.S., Green lubricants, Environmental benefits and impacts of lubrication, Green Chemistry, **4**, 2002, 293-307.
7.HUTCHINGS I., Lubricants and lubrication - ScienceDirect. Tribology (Second Edition), **978**, 2017, 79-105.
8.LI JS., ZHANG L., WANG.H.D., Research status and development trend of Nanoparticles as lubricating oil additives, Lubricating Oil, **01**, 2008,5-9.
9.HONG H., ROY W., Heat transfer nanolubricant and nanogrease based on carbon nanotube, Proceedings of Spie the International Society for Optical Engineering, **2**, 2006,133-138.
10.LI JS., HAO LF., et al., Preparation, Characterization and Tribological Evaluation of Calcium Borate Nanoparticles as Lubricant Additives[J], Journal of Chromatography A, **148**, 2010, 1047-1056.
11.YU HL., XU Y., et al., Tribological properties and lubricating mechanisms of Cu nanoparticles in lubricant. Transactions of Nonferrous Metals Society of China, **18**, 2008, 636-641.
12.SHEN G., ZHENG Z., WAN Y., et al., Hydrolytic stability and triboligical properties of organic borate esters as lubricant additives[J], Journal of Tsinghua University (Science and Technology),**10**, 1999, 97-100.

13.QIAO Y., ZHAO H., YAN Z., et al., Research progress of functionalization modifition and applications of graphene as lubricating additive, Chemical Industry and Engineering Progress. **33**, 2014, 216-223.
14.HUANG G., CHEN Z., LI M., Surface Functional Modification of Graphene and Graphene Oxide, Acta Chimica Sinica, **74**, 2016, 789-799.
15. PU JB., WANG LP., XUE QJ., Progress of Tribology of Graphene and Graphene-based Composite Lubricating Materials. Tribology, **34**, 2014, 93-112.
16.HADDAD SA, et al., SiO_2-covered graphene oxide nanohybrids for in situ preparation of UHMWPE/GO(SiO_2) nanocomposites with superior mechanical and tribological properties, Journal of Applied Polymer Science, **136**, 2019, 477-496.
17.GUO P., CHEN L., WANG J., et al., Enhanced Tribological Performance of Aminated Nano-Silica Modified Graphene Oxide as Water-Based Lubricant Additive, ACS Applied Nano Materials. **1**,2018, 6444-6453.
18.TITELMAN GI, et al., Characteristics and microstructure of aqueous colloidal dispersions of graphite oxide. Carbon., **43**, 2005, 641-649.
19.PARK S., RUOFF RS., Chemical methods for the production of graphenes, Nature Nanotechnology, **5**, 2010, 309-322.
20.MATSUO Y., SUGIE Y., Preparation, structure and electrochemical property of pyrolytic carbon from graphite oxide, Carbon, **36**, 1998, 301-303.
21.MARCANO DC., KOSYNKIN DV., et al., Improved synthesis of graphene oxide. Acs Nano, **4**, 2010, 4806-4814.
22.HA T., VU T., THUY T., et al., Solvothermal synthesis of Pt-SiO_2/graphene nanocomposites as efficient electrocatalyst for methanol oxidation[J], Electrochimica Acta, **161**, 2015, 335-342.
23.RIO J., LOPEZ E., et al., Tribological properties of graphene nanoplatelets or boron nitride nanoparticles as additives of a polyalphaolefin base oil. Journal of Molecular Liquids, **333**, 2021, 115-119.
24.ZHANG YT., LI K., et al., Synthesis and photocatalytic CO_2 reduction activity of a coal-based graphene assembly, Carbon, **104**, 2016, 261.
25.YANG Y., LIU T., Fabrication and characterization of graphene oxide/zinc oxide nanorods hybrid. Applied Surface Science, **257**, 2011, 8950-8954.
26.NETHRAVATHI C., RAJAMATHI M., Chemically modified graphene sheets produced by the solvothermal reduction of colloidal dispersions of graphite oxide, Carbon, 46, 2008,1994-1998.
27.ARMANO A., BUSCARINO G., et al., Graphene-SiO_2 Interaction from Composites to Doping, physica status solidi A, **216**, 2019, 1-11.
28.POURHASHEM, SEPIDEH, et al., Investigating the effect of SiO_2-graphene oxide hybrid as inorganic nanofiller on corrosion protection properties of epoxy coatings, Surface & Coatings Technology, **311**, 2017, 282-294.
29.ZENG H., YI GY., XING B., et al., Preparation of coal-based graphene/TiO_2 composites and their photocatalyticactivity, Chemical Industry and Engineering Progress, **36**, 2017, 2568-2576.
30.ZHOU Q., ZHAO Z., ZHANG Y., et al., Graphene Sheets from Graphitized Anthracite Coal: Preparation, Decoration, and Application. Energy & Fuels, **26**, 2012, 5186–5192.
31.KIM CY, KIM SH, et al., Characteristics of low-k SiOC(-H) films deposited at various substrate temperature by PECVD using DMDMS/O_2 precursor. Thin Solid Films, **516**, 2007,340-344.
32.DONG R., WANG L., et al., A novel SiO_2-GO/acrylic resin nanocomposite: fabrication, characterization and properties, Applied Physics A., **125**, 2019, 1-11.
33.MA SY., ZHENG SH., et al., Anti-Wear and Reduce-Friction Ability of ZrO_2/SiO_2 Self-Lubricating Composites, Advanced Materials Research, **79**, 2009, 1863-1866.

34.WANG R., WU Q., et al., Dispersion stability of nano-$NiFe_2O_4$ powders in refrigeration lubricant oil, Huagong Xuebao/CIESC Journal, 61, 2010, 1-8.
35.QI FY., HUANG QY., et al., Characterization of N719 Dye Desorption on TiO_2 Nanotube Arrays Used for Dye-Sensitized Solar Cells, Advanced Materials Research, **631**, 2013, 524-529.

Manuscript received: 26.02.2022